ChemPubSoc Europe
DOI: 10.1002/cctc.201801626
CHEMCATCHEM
Full Papers

Fe/Fe_2O_3@N-dopped Porous Carbon: A High-Performance Catalyst for Selective Hydrogenation of Nitro Compounds

Ruirui Yun,*[a] Lirui Hong,[a] Wanjiao Ma,[a] Weiguo Jia,[a] Shoujie Liu,*[a] and Baishu Zheng*[b]

Herein, we designed and prepared a novel Fe/Fe_2O_3-based catalyst, in which a remarkable synergistic effect has been revealed between Fe and Fe_2O_3 encapsulated in N-doping porous carbon. The Fe-based catalysts were fabricated *via* pyrolysis a mixture of MIL-101(Fe) and melamine. The catalyst exhibits exceptionally high catalytic activity (TOFs up to 8898 h^{-1} which is about 100 times higher than the similar kinds of catalysts) and chemoselectivity for nitroarene reduction under mild conditions.

Introduction

Catalysis is a core field of material science due to their widely application in modern chemistry.[1] Selectivity and catalyst separation are major issue in heterogeneous catalysis.[2] In particular, the chemoselective hydrogenation of functionalized nitro compounds to amine is an industrially important transformation, principally in the agrochemical, pigment and pharmaceutical industries.[3] Achieving high selectivity along with high conversion has emerged as the prime concern in designing catalysts. Consequently, much more methods have been applied to obtain highly efficient catalysts, such as doping heteroatom and bimetallic synergistic effect.[4]

In terms of industrial applications, heterogeneous catalysts instead of homogeneous ones attract more and more attentions due to the ease of their separation and recycling.[5] However, various metal catalysts based on noble metal-based (for example, Pd, Pt, Au, Ru, *etc.*) are often not chemoselective.[6] Therefore, the heterogeneous catalysts based upon earth-abundant metal, such as Fe, Co, and Ni, have been devoted to designing.[7] Although earth-abundant metals are low-cost, sintering or leaching of them cause irreversible deactivation of the catalysts under liquid phase conditions, so new strategies have been designed to fabricate stable, high active, and selective earth-abundant metal catalysts are very necessary.

In the past decades, much attention has been paid to develop heteroatom decorated porous carbon materials which considerably broadens their potential applications. Among various possible dopants, nitrogen-containing nanostructured carbon materials are potentially of great technological interest for the development of a catalytic system.[8] It is widely accepted that the nitrogen atoms in metal modified N-doping carbon catalysts act as base sites which could increase the performance of hydrogenation of nitro compounds.[9] Additionally, to obtain efficient and stable metal-base catalysts, having base metal nanoparticles (NPs) with small sizes stabilized inside a stable porous matrix would be an ideal strategy. In the previous studies, much more attention has been focused on Zeolitic imidazolate frameworks (ZIFs),[10] which fabricated by imidazole and metal ions can be pyrolyzed to obtain N-doping porous carbon.[11] However, up to now, the less nitrogen content of the N-doping porous carbon limits its application.

For this purpose, metal-organic frameworks (MOFs),[12] the same as ZIFs, are a novel class of porous materials with polyhedral cage, abundant carbon and high metal ion contents and are expected to be good candidates as the precursor template to design various porous nanostructured metal oxide hybrid materials.[13] Therefore, a new strategy, which pyrolyze the mixture of MOFs and N-contain organic ligands, to obtain tolerant catalyst was sought that would minimize reaction times and have high chemoselectivity.

The MIL-101 (Fe) was solvothermally synthesized based upon $Fe(NO_3)_3{\cdot}6H_2O$ and terephthalic acid in DMF solution. The structure and phrase purity of MIL-101(Fe) have been confirmed by powder X-ray diffraction (XRD) (Figure S1, ESI). The catalysts Fe/Fe_2O_3@N^nPC-T-X (n represent the ratio of MIL-101 (Fe) and melamine, T represent pyrolysis temperature and x represent pyrolysis time; n = 0, 1, 2, 3, 4, 5, 6; T = 600 °C, 700 °C, 800 °C; x = 1 h, 2 h, 3 h) were prepared in sequential pyrolysis procedure in an Ar atmosphere (Figure 1, see details in the ESI). Catalysts optimization studies revealed a dependence on the three key variables: (1) the ratio of MIL-101 (Fe) and melamine, (2) the pyrolysis temperature, and (3) the time of pyrolysis. As Powder X-ray diffraction patterns indicate the composition of the products obtained at different temperature displays distinct differences while the different ratio and time are not (Figure S2,

---

[a] *Prof. R. Yun, L. Hong, W. Ma, W. Jia, Dr. S. Liu*
The Key Laboratory of Functional Molecular Solids
Ministry of Education
College of Chemistry and Materials Science
Anhui Normal University
Wuhu 241000 (P. R. China)
E-mail: ruirui58@ahnu.edu.cn
sjliu@ahnu.edu.cn
[b] *Prof. Dr. B. Zheng*
Key Laboratory of Theoretical Organic Chemistry and Function Molecule
Ministry of Education
Hunan Provincial Key Laboratory of Controllable Preparation and Functional Application of Fine Polymers
School of Chemistry and Chemical Engineering
Hunan University of Science and Technology
Xiangtan 411201 (P. R. China)
E-mail: zbaishu@163.com

Supporting information for this article is available on the WWW under https://doi.org/10.1002/cctc.201801626

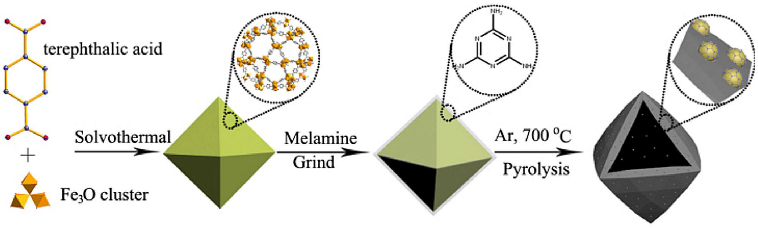

Figure 1. Schematic illustration of the preparation of Fe/Fe_2O_3@N^nPC-700-x.

S3, S4, ESI). It is interesting that all peaks for Fe/Fe_2O_3@N^5PC-600-1 can be indexed to the phase of Fe_3C (JCPDS N0.76-1877), while the temperature over 600 °C the Fe_3C change to Fe/Fe_2O_3 (CPDS N0.06-0696/JCPDS N0.39-1346), such as Fe/Fe_2O_3@N^nPC-700-1 and Fe/Fe_2O_3@N^5PC-800-1 (Figure S2, S3). Moreover, the powder XRD patterns of Fe/Fe_2O_3@N^nPC-700-x, Fe is the major product, accompanied by portions of Fe_2O_3 while no sign of Fe_3C can be found.

Results and Discussion

Characterization of the Fe-Based Catalysts

The microstructure observation using scanning electron microscopy (SEM) suggests that MIL-101 (Fe) microcrystals are of uniform octahedral (Figure 2a). After pyrolysis up to 600 °C, its shape is collapsed, however the shape is almost retained while the mixture melamine and MIL-101 (Fe) are heated up to 600~800 °C (Figure 2b). As shown in the transmission electron microscope (TEM) and high-resolution TEM image for Fe/Fe_2O_3@N^5PC-700-1, high density small nanoparticles (NPs) are uniform distributed and coated with N-doping porous carbon (Figure 2c, d).

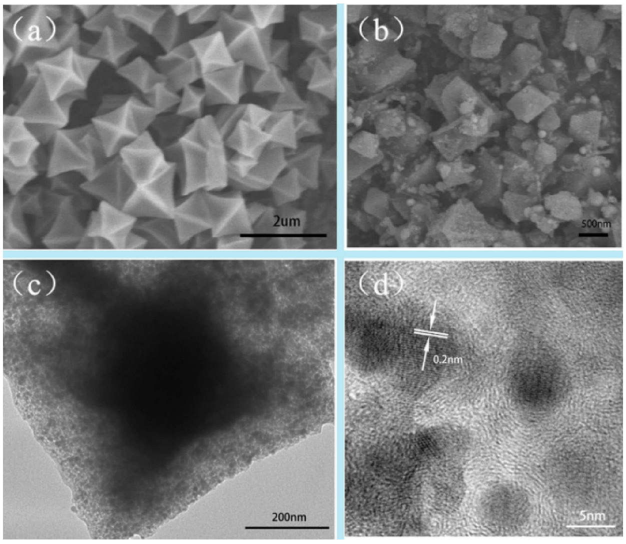

Figure 2. Microstructure observation for MIL-101 (Fe) and Fe/Fe_2O_3@N^nPC-700-1. (a) SEM images of MIL-101 (Fe) and (b) Fe/Fe_2O_3@N^nPC-700-1. (c) TEM and (d) HRTEM images of Fe/Fe_2O_3@N^nPC-700-1.

X-ray photoelectron spectroscopy (XPS) was carried out to further investigate the surface compositions and chemical state of the Fe/Fe_2O_3@N^5PC-700-1. As shown in Figure S7 (ESI), the Fe 2p exhibits two broad peaks at 706.75, 710.1, 719.95 and 723.7 eV, corresponding to Fe $2p_{3/2}$ and $2p_{1/2}$, respectively. Their separation $\Delta_1 = 719.95–706.75 = 13.2$ eV and $\Delta_1 = 723.7–710.1 = 13.6$ eV, are similar to Fe and Fe_2O_3, respectively, which is supported by the powder XRD results. All these characterization results clearly suggest that the pyrolysis of the mixture of melamine and MIL-101 (Fe) lead to well dispersed Fe/Fe_2O_3 is encapsulated in N-doping porous carbon.

The formation change of graphitic carbon caused by temperature was further studied by Raman spectroscopy (Figure S8), in which two distinct bands at ~1345 cm^{-1} and 1590 cm^{-1} can be assigned to the defective/disordered sp^3 hybridized carbon (D band) and the crystallized graphitic sp^2 carbon (G band), respectively. The decrease of I_D/I_G relative ratio from 1.01 to 0.84 also confirms improved graphitic nature after elevated temperature. The defection of carbon is expected to favor rapid mass-transfer and can provide sufficient active site exposure for catalysis.

The obtained catalysts were investigated for catalytic reduction of functionalized nitro compounds in the presence of hydrazine hydrate as hydrogen source. Transfer hydrogenation of 1-bromo-4-nitrobenzene was chosen as a benchmark reaction. We can see from the Figure 3, it is notable that heteroatom N-doping in the carbon framework of the catalysts remarkably boosted the reaction efficiency. The catalyst Fe/Fe_2O_3@ N^0PC-700-1 gave lower desired products. In contrast, the catalyst Fe/Fe_2O_3@N^1PC-700-1 show 34.8% conversion which is 3 times higher than that of Fe/Fe_2O_3@N^0PC-700-1 under identical conditions. Additionally, the conversion is increased accompany with the amount of N-doping, especially the catalyst of Fe/Fe_2O_3@N^5PC-700-1 achieves the maximum performance. The catalytic results clearly indicate that the N heteroatom in the framework resulting the component of the catalyst changing which may play a vital role in the reduction (Fig. S2). In addition, the size distribution of Fe/Fe_2O_3 NPs was smaller, and the dispersity was more uniform when the ratio of melamine is increased to 5 (Figure S10). On the other hand, among different pyrolysis temperatures, 700 °C is best one of 600 °C and 800 °C. It seems that the prolonged pyrolysis time is also not beneficial

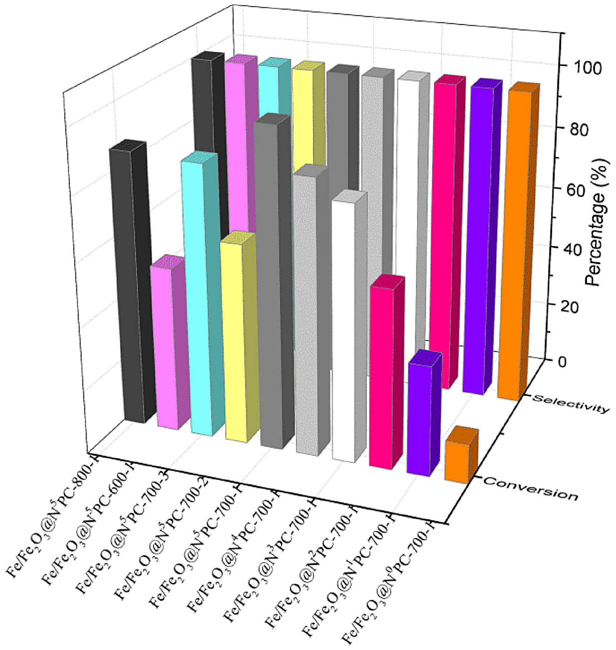

Figure 3. The conversion and selectivity for hydrogenation of bromo-4-nitrobenzene with different catalysts (note: Fe/Fe$_2$O$_3$@N^{0}PC-700-1 namely as MIL-101 pyrolysis without melamine).

for the activity, may because of the component changed when the temperature at 600 °C and 800 °C (Figure S3).

Encouraged by the superb performance of Fe/Fe$_2$O$_3$@N^{5}PC-700-1, the hydrogenation of a variety of nitro compounds were carried out. As shown in Table 1, in general, the catalyst enabled the reduction of various functionalized nitro compounds, yield the corresponding substituted aromatic anilines with high conversions and selectivities. Electron-donating and electron-withdrawing substituent at *o*-, *m*-, *p*-positions on the phenyl ring of nitro compounds gave high conversion. More importantly, for halogenated nitrobenzenes, giving excellent yields of the target products without dehalogenation processes. To our delight, the catalyst shows high chemoselectivity in the reduction of substituted nitroarenes with quite challenging reducible functional groups, such as carboxyl, carbonyl, ester, and cyano (entries 13–15), giving the corresponding anilines derivatives in >99% yield without any byproducts. This remarkable result highlights the chemoselectivity of this Fe-based nanocatalyst, displaying excellent advantage compared to that of noble metal-based catalysts. Subsequently, we turned our interest towards nitrocyclohexane (entry 16). Interestingly, nitrocyclohexane was reduced to cyclohexylamine with high conversion, which manifest that the Fe/Fe$_2$O$_3$@N^{5}PC-700-1 is effective for the hydrogenation both of nitroarenes and nitro-aliphatic hydrocarbon.

Durability and recyclability of catalyst are critical for practical applications.[15] To demonstrate the stability and

Table 1. Hydrogenation of different nitro compounds by Fe/Fe$_2$O$_3$@N^{5}PC-700-1.

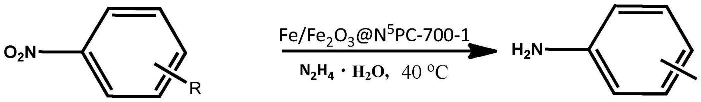

Entry	Substrate	Time [h]	Conv.[a] [%]	Select.[a] [%]	Entry	Substrate	Time [h]	Conv.[a] [%]	Select.[a] [%]
1	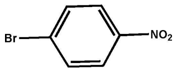	0.3	100	>99	9	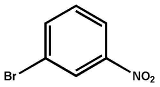	0.3	100	>99
2	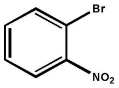	0.5	100	>99	10	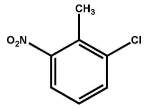	0.5	100	>99
3	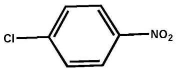	0.3	100	>99	11	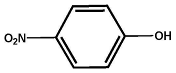	0.5	100	>99
4	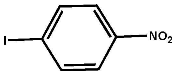	0.3	100	>99	12	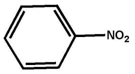	0.3	100	>99
5	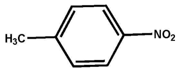	0.3	100	>99	13	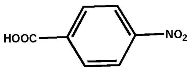	0.3	100	>99
6	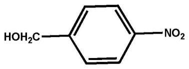	0.5	100	>99	14	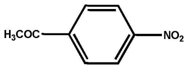	0.3	100	>99
7	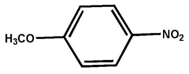	0.3	100	>99	15	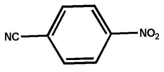	0.3	100	99
8	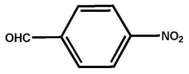	0.3	100	>99	16	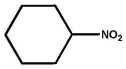	1	100	>90

[a] Determined by GC methods with *n*-dodecane as standard.

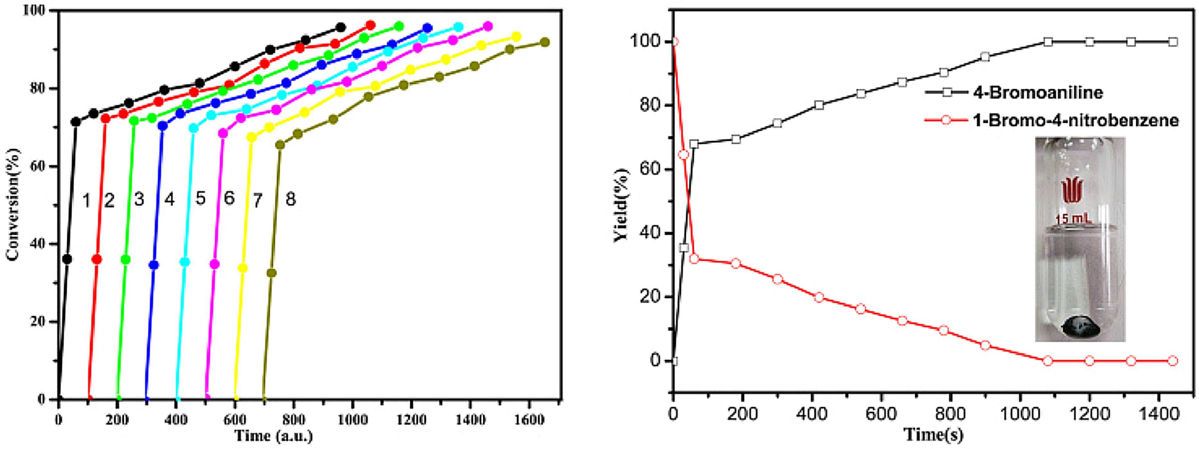

Figure 4. Recyclability tests of $Fe/Fe_2O_3@N^5PC$-700-1; Right: conversion of 1-bromo-4-nitrobenzen to 4-bromoaniline (inset, the facile separation of the catalyst via magnet).

reusability of $Fe/Fe_2O_3@N^5PC$-700-1, as shown in Figure 4, recycling experiments for the hydrogenation of 1-bromo-4-nitrobenzene were conducted (the detail can be found in experimental section). Powder XRD observation clearly demonstrated the maintained the phase composition of $Fe/Fe_2O_3@N^5PC$-700-1 after recycling (Figure S5, ESI). Additionally, the used catalyst is easily separated by magnet due to the strong magnetism of $Fe/Fe_2O_3@N^5PC$-700-1 (Figure 4 right inset).

Conclusions

In summary, we developed heterogeneous, low-cost, magnetically recyclable, and highly efficient Fe-based NPs encapsulated with a N-doping porous carbon derived from pyrolysis melamine. The synergism of N dopant on the porous carbon and confined Fe NPs produces highly active sites for catalytic transfer hydrogenation of functionalized nitro compounds under mild conditions. The Fe-based catalyst is readily recycled with a magnet and can be reused at least six times without any loss of activity. This study provides a new way to introduce highly dispersed active metal/metal oxide species encapsulated in heteroatom doping porous carbon and improved performance toward diverse catalytic reactions.

Experimental Section

Preparation of Catalysts

Synthesis of MIL-101 (Fe): Iron(III) nitrate hexahydrate (0.5 g) was dissolved in 5 mL of methanol, and 1,4-terephthalic acid (2 g) was dissolved in 15 mL of methanol. The above solutions were mixed together and stirring for 4 hours under 100 °C. The resulting yellow precipitates were harvested by centrifuging, washing with methanol, and finally being dried in vacuum at 40 °C overnight.

Preparation of $Fe/Fe_2O_3@N^nPC$-T-x: The powder of MIL-101 and melamine were placed in a quartz mortar. Then the mixture in mortar was uniformly ground. The resulting mixture was then placed in a tube furnace under Ar gas flow of about 50 mL/min, was pyrolyzed from room temperature to the targeted temperature (600 °C ~ 800 °C) at a heating rate of 5 °C/min. After the temperature reached the target temperature and maintained for 1 ~ 3 hours, the resulting product was cooling down to the room temperature naturally. The resultant samples were denoted as $Fe/Fe_2O_3@N^nPC$-T-x (n represent the ratio of MIL-101 (Fe) and melamine, T represent pyrolysis temperature and x represent pyrolysis time).

Catalytic Performance Evaluation

The reduction of bromo-4-nitrobenzene: Typically, the catalyst (0.025 mmol) was charged into a dried round bottom flask with 10 mL ethanol. Then 100 mg bromo-4-nitrobenzene (1 mmol) and 2 mL hydrazine hydrate (40 mmol) were added sequentially. Then the mixture was heated 40 °C with 18 min. The conversion and selectivity were detected by GC-MS with n-dodecane as standard.

Recyclability investigation for $Fe/Fe_2O_3@N^5PC$-700-1 catalyst: The catalyst (0.0125 mmol) was used to hydrogenation of 1-bromo-4-nitrobenzene (1 mmol). Sampling analysis is performed for fixed times (30 s, 60 s, 120 s, 240 s, 360 s, 480 s, 600 s, 720 s, 840 s, 960 s). After the reduction of 1-bromo-4-nitrobenzene for 20 min, the catalyst was separated out by an external magnet. Then the recovered catalyst was washed by ethanol for several times. After that, the catalyst was used by another reduction of fresh bromo-4-nitrobenzene. This procedure was conducted five times to examine the recyclability of $Fe/Fe_2O_3@N^5PC$-700-1, and the selectivity and conversion were detected by GC-MS with n-dodecane as standard.

The reduction of variety of nitro compounds: In a particular reaction, Fe-based catalysts (0.025 mmol) were put into a dried round bottom flask with 10 mL solvent. Sequentially, 100 mg nitro compounds (1 mmol) and 2 mL hydrazine hydrate (40 mmol) were added. Then the mixture was heated 40 °C with 0.3 hour. The selectivity and conversion were detected by GC-MS with n-dodecane as standard.

Acknowledgements

This work was supported by the National Natural Science Foundation of China (NSFC: 21401004, 21201062), the Natural Science Foundation of Anhui Province (1508085QB36), the Doctoral Scientic Research Foundation (070138).

Conflict of Interest

The authors declare no conflict of interest.

Keywords: Fe-based catalyst · N-doped porous carbon · Chemoselectivity · Nitro compounds

[1] a) Y. Wang, Z. Huang, X. Leng, H. Zhu, G. Liu, Z. Huang, *J. Am. Chem. Soc.* **2018**, *140*, 4417–4429; b) Y. Duan, T. Song, X. Dong, Y. Yang, *Green Chem.* **2018**, *20*, 2821–2828.
[2] a) J. Jia, C. Qian, Y. Dong, Y. F. Li, H. Wang, M. Ghoussoub, K. T. Butler, A. Walsh, G. A. Ozin, *Chem. Soc. Rev.* **2017**, *46*, 631–4644; b) T. Osako, K. Torii, S. Hirata, Y. Uozumi, *ACS Catal.* **2017**, *7*, 7371–7377; c) Y. Cao, S. Mao, M. Li, Y. Chen, Y. Wang, *ACS Catal.* **2017**, *7*, 8090–8112.
[3] a) J. Camacho-Bunquin, M. Ferrandon, H. Sohn, D. Yang, C. Liu, P. A. I. Leon, F. A. Perras, M. Pruski, P. C. Stair, M. Delferro, *J. Am. Chem. Soc.* **2018**, *140*, 3940–3951; b) P. G. Andersson, I. J. Munslow, *Modern Reduction Methods*, Wiley-VCH Verlag GmbH & Co. KGaA: Weinheim, **2008**.
[4] a) H. Pang, F. Gallou, H. Sohn, J. Camacho-Bunquin, M. Delferro, B. H. Lipshutz, *Green Chem.* **2018**, *20*, 130–135; b) S. De, J. Zhang, R. Luque N. Yan, *Energy Environ. Sci.* **2016**, *9*, 3314–3347; c) D. R. Pye N. P. Mankad, *Chem. Sci.* **2017**, *8*, 1705–1718; d) Y. Peng, Z. Geng, S. Zhao, L. Wang, H. Li, X. Wang, X. Zheng, J. Zhu, Z. Li, R. Si, J. Zeng, *Nano Lett.* **2018**, *18*, 3785–3791; e) J. Song, Z.-F. Huang, L. Pan, K. Li, X. Zhang, L. Wang J.-J. Zou, *Appl. Catal. B: Environ.* **2018**, *227*, 386–408.
[5] a) A. M. Tafesh, J. Weiguny, *Chem. Rev.* **1996**, *96*, 2035–2052; b) J. Kou, C. Lu, J. Wang, Y. Chen, Z. Xu, R. S. Varma, *Chem. Rev.* **2017**, *117*, 1445–1514.
[6] a) S. Byun, Y. Song, B. M. Kim, *ACS Appl. Mater. Interfaces*, **2016**, *8*, 14637–14647; b) Á. Vivancos, M. Beller, M. Albrecht, *ACS Catal.* **2018**, *8*, 17–21; c) F. Meemken, A. Baiker, *Chem. Rev.* **2017**, *117*, 11522–11569.
[7] a) R. V. Jagadeesh, G. Wienhöfer, F. A. Westerhaus, A.-E. Surkus, M.-M. Pohl, H. Junge, K. Junge, M. Beller, *Chem. Commun.* **2011**, *47*, 10972–10974; b) R. V. Jagadeesh, A.-E. Surkus, H. Junge, M.-M. Pohl, J. Radnik, J. Rabeah, H. Huan, V. Schünemann, A. Brückner, M. Beller, *Science* **2013**, *342*, 1073–1076; c) R. Ma, Z. Chen, F. Cao, S. N. Wang, X. Huang, Y. Li, J. Lu, D. Li, J. M. Dou, *Dalton Trans.* **2017**, *46*, 2137–2145; d) X. Ma, Y.-X. Zhou, H. Liu, Y. Li, H.-L. Jiang, *Chem. Commun.* **2016**, *52*, 7719–7722; e) J. R. Morse, J. F. Callejas, A. J. Darling, R. E. Schaak, *Chem. Commun.* **2017**, *53*, 4807–4810; f) Y. Zhu, S. Yang, C. Cao, W. Song L.-J. Wan, *Inorg. Chem. Front.* **2018**, *5*, 1094–1099; g) S. Yang, L. Peng, D. T. Sun, E. Oveisi, S. Bulut, W. L. Quee, *ChemSusChem*, **2018**, *11*, 3131–3138.
[8] a) A. Grirrane, A. Corma, H. Garcia, *Science*, **2008**, *322*, 1661–1664; b) X.-K. Kong, Z.-Y. Sun, M. Chen, C. Chen, Q.-W. Chen, *Energy Environ. Sci.* **2013**, *6*, 3260–3266; c) Z. Wei, J. Wang, S. Mao, D. Su, H. Jin, Y. Wang, F. Xu, H. Li, Y. Wang, *ACS Catal.* **2015**, *5*, 4783–4789.
[9] a) X. Wang, Y. W. Li, *J. Mol. Catal. A* **2016**, *420*, 56–65; b) P. Zhou, Z. H. Zhang, L. Jiang, C. L. Yu, K. L. Lv, J. Sun, S. G. Wang, *Appl. Catal. B*, **2017**, *210*, 522–532; c) X. M. Liu, S. J. Cheng, J. L. Long, W. Zhang, X. H. Liu, D. P. Wei, *Mater. Chem. Front.* **2017**, *1*, 2005–2012.
[10] A. Phan, C. J. Doonan, F. J. Uribe-Romo, C. B. Knobler, M. O'Keeffe, O. M. Yaghi, *Acc. Chem. Res.* **2010**, *43*, 58–67.
[11] a) Y. Pan, K. Sun, S. Liu, X. Cao, K. Wu, W.-C. Cheong, Z. Chen, Y. Wang, Y. Li, Y. Liu, D. Wang, Q. Peng, C. Chen, Y. Li, *J. Am. Chem. Soc.* **2018**, *140*, 2610–2618; b) F.-Y. Yi, R. Zhang, H. Wang, L.-F. Chen, L. Han, H.-L. Jiang, Q. Xu, *Small Methods*, **2017**, *1*, 1700187.
[12] a) H.-C. Zhou, J. R. Long, O. M. Yaghi, *Chem. Rev.* **2012**, *112*, 673; b) H.-C. Zhou, S. Kitagawa, *Chem. Soc. Rev.* **2014**, *43*, 5415; c) Z. Zhang, M. J. Zaworotko, *Chem. Soc. Rev.* **2014**, *43*, 5444–5455; d) Q. Yang, Q. Xu, H.-L. Jiang, *Chem. Soc. Rev.* **2017**, *46*, 4774–4808.
[13] a) J. Tang, R. R. Salunkhe, J. Liu, N. L. Torad, M. Imura, S. Furukawa, Y. Yamauchi, *J. Am. Chem. Soc.* **2015**, *137*, 1572–1580; b) M. S. Denny, L. R. Parent, J. P. Patterson, S. K. Meena, H. Pham, P. Abellan, Q. M. Ramasse, F. Paesani, N. C. Gianneschi, S. M. Cohen, *J. Am. Chem. Soc.* **2018**, *140*, 1348–1357; c) T. Wang, H.-K. Kim, Y. Liu, W. Li, J. T. Griffiths, Y. Wu, S. Laha, K. D. Fong, F. Podjaski, C. Yun, R. V. Kumar, B. V. Lotsch, A. K. Cheetham, S. K. Smoukov, *J. Am. Chem. Soc.* **2018**, *140*, 6130–6136; d) H. Chen, K. Shen, Q. Mao, J. Chen, Y. Li, *ACS Catal.* **2018**, *8*, 1417–1426.
[14] a) Y. Li, Y.-X. Zhou, X. Ma, H.-L. Jiang, *Chem. Commun.* **2016**, *52*, 4199–4202; b) M. Tian, X. Cui, M. Yuan, J. Yang, J. Ma, Z. Dong, *Green Chem.* **2017**, *19*, 1548–1554; c) Y. Jang, S. Kim, S. W. Jun, B. H. Kim, S. Hwang, I. K. Song, B. M. Kim, T. Hyeon, *Chem. Commun.* **2011**, *47*, 3601–3603.
[15] a) F. Schüth, M. D. Ward, J. M. Buriak, *Chem. Mater.* **2018**, *30*, 3599–3600; b) S. L. Scott, *ACS Catal.* **2018**, *8*, 8597–8599.

Manuscript received: October 8, 2018
Revised manuscript received: November 22, 2018
Version of record online: [redacted], [redacted]

FULL PAPERS

Catalysis magic! Fe-based NPs catalyst encapsulated in N-doping porous carbon exhibits high catalytic active (with TOF = 8898 h^{-1} which is about 100 of times higher than the similar catalysts) and chemoselectivity for nitro compounds reduction.

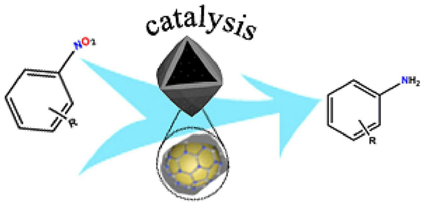

Prof. R. Yun, L. Hong, W. Ma, W. Jia, Dr. S. Liu*, Prof. Dr. B. Zheng**

1 – 6

Fe/Fe$_2$O$_3$@N-dopped Porous Carbon: A High-Performance Catalyst for Selective Hydrogenation of Nitro Compounds